Electronic Supplementary Material (ESI) for Physical Chemistry Chemical Physics.
This journal is © the Owner Societies 2020

Supporting Information

Precursor Chemistry of h-BN: Adsorption, Desorption, and Decomposition of Borazine on Pt(110)

Leander Haug[†], Jannik P. Roth[‡], Marco Thaler[†], Dominik Steiner[†], Alexander Menzel[†], Sergio Tosoni[‡], Gianfranco Pacchioni[‡], and Erminald Bertel[†]

[†]Institute of Physical Chemistry, University of Innsbruck, Innrain 52c, 6020 Innsbruck, Austria

[‡] Dipartimento di Scienza dei Materiali, Università Milano-Bicocca, Via R. Cozzi 55, 20125 Milan, Italy

Contents:

1. Geometry and orbital structure of gas phase Borazine:

	this work	Exp.[1]
$d_{B\text{-}N}$ [Å]	1.434	1.4355 ± 0.0021
$d_{B\text{-}H}$ [Å]	1.202	1.258 ± 0.014
$d_{N\text{-}H}$ [Å]	1.016	1.050 ± 0.012
$\angle_{NBN}$ [°]	116.9	117.7 ± 1.2
$\angle_{BNB}$ [°]	123.1	121.1 ± 1.2

Table ST1: Geometry of gas phase Borazine obtained in the present DFT calculation and comparison to experimental data[1].

Table ST2 shows the structure, the energies and the bonding character of the occupied Borazine molecular orbitals obtained from the DFT calculations in comparison to the results of a molecular orbital configuration interaction calculation (MO CI)[2].

DFT (this work)				MO CI[2]		
	charge density	E_{rel} [eV]	description	symmetry	description	E_{rel} [eV]
HOMO	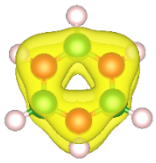	0	π-BN	1e''	π-BN, N dominant	0
HOMO-1	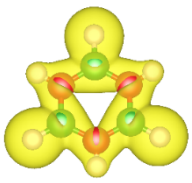	-0.828	BH bonds	6e'	BH bonds	-1.41
HOMO-2	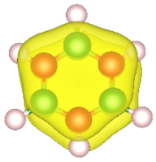	-2.125	π-BN	$1a_2$''	π-BN, N dominant	-2.95
HOMO-3	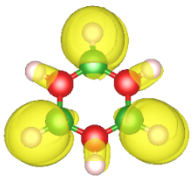	-2.478	BH bonds	$5a_1$'	BH bonds	-4.08
HOMO-4	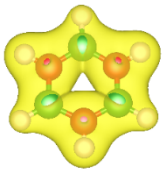	-3.805	σ-BN, NH/BH	$1a_2$'	BN	-5.09
				5e'	NH bonds	-5.45
HOMO-5	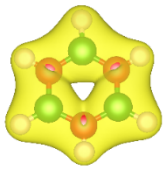	-6.095	σ-BN, NH/BH	4e'	BN	-8.75
HOMO-6	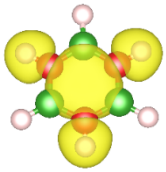	-6.865	NH bonds	4a1'	NH bonds	-9.08

Table ST2: Structure and binding energies of the occupied Borazine MOs in the gas phase. Note the reduced energy spread of the energy levels in the DFT calculations as compared to MO CI results. Colour code: N red, B green, H pink.

2. The transition from mono- to multilayer as seen by TPD:

Figure S1 shows a selection of mass 80 TPD spectra around the transition from monolayer coverage to multilayer coverage. Coverages up to monolayer completion are characterized by second-order desorption, coverages beyond the monolayer by zero-order desorption. The TPD obtained after an exposure of 17 L is unique: It is a member of the second-order desorption family as demonstrated by the nearly perfect second-order fit, but simultaneously it has a leading edge in line with the zero-order TPDs obtained after higher exposures. Therefore it is attributed to desorption from the saturated monolayer. The small deviation of the leading edge from the second-order fit (see figure 1 in the main text) could indicate incipient second-layer coverage. Since the leading edge remains identical for all higher coverages, one can conclude that the second layer has already lost memory of the substrate and experiences the same interaction with the support as the higher layers. Given that there is no preferred orientation in the multilayer, this indicates the presence of different orientations in the monolayer as well.

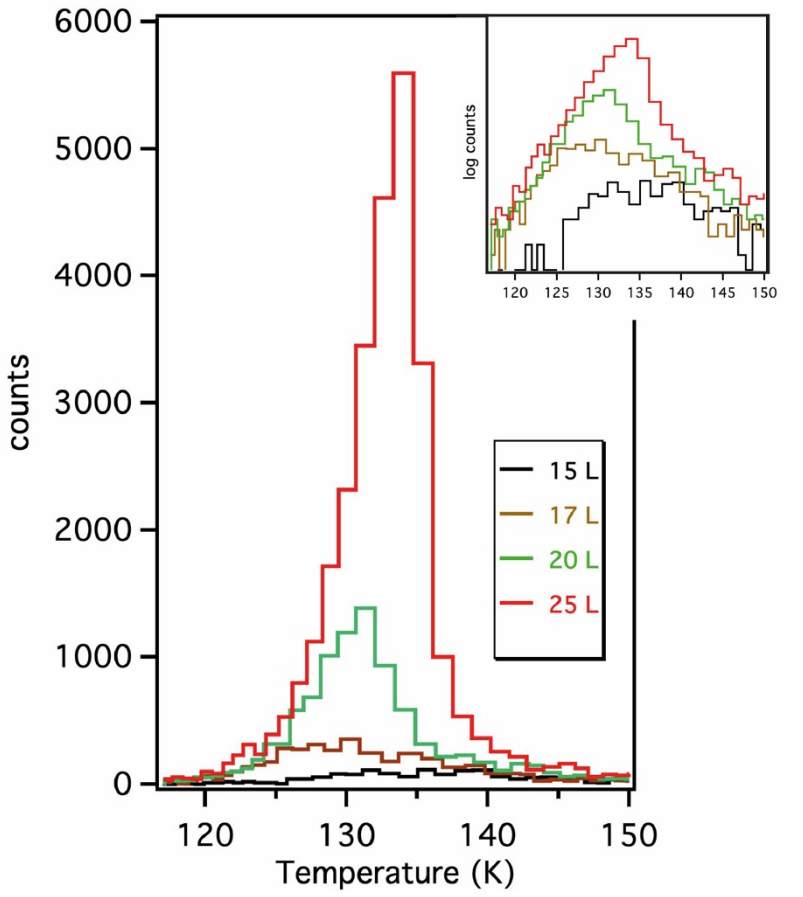

Figure S1: Selected TPD spectra for exposures below and above monolayer saturation. The insert shows the same spectra on a logarithmic scale.

3. Comparison of the H_2 desorption spectra from Pt(111) and Borazine/Pt(111):

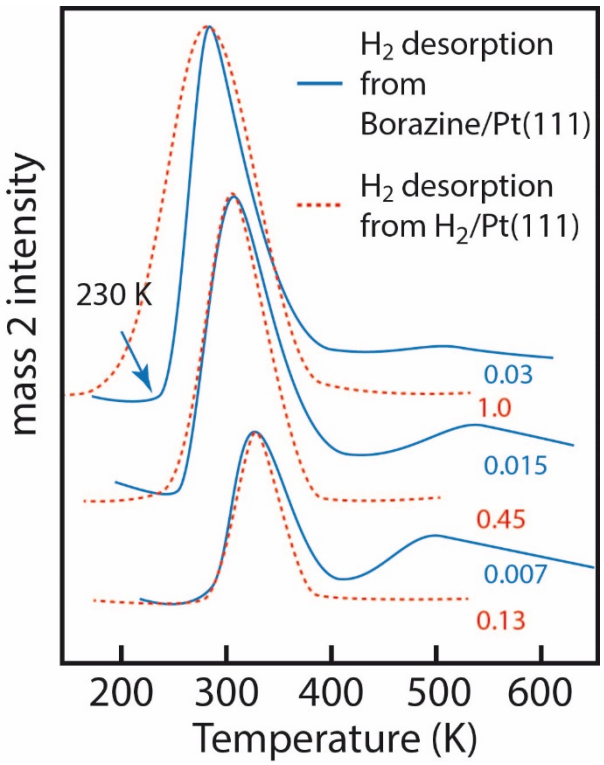

Figure S2: Blue curves show TPD traces of H_2 from Borazine/Pt(111)[3]. The index refers to the Borazine exposure. Red dotted curves are TPD traces for H_2/Pt(111)[4]. Here, the index refers to relative coverage θ_H, where θ_H = 1 corresponds to the coverage obtained after 3000 (Torr × s) exposure.

The TPD spectra of H_2 from Borazine/Pt(111)[3] are strikingly similar to those from H_2/Pt(111)[4] with one exception, namely the delayed onset of the desorption peak from Borazine/Pt(111) at the highest coverage shown in Fig. S2. This allows the following conclusions: For temperatures above 230 K, dehydrogenation of Borazine is not the rate-limiting step. Rather, H atoms liberated from adsorbed Borazine desorb from Pt(111) in much the same way as if there were no co-adsorbates. With increasing coverage, however, the H_2 desorption peak shifts to successively lower temperatures, as expected for second-order desorption kinetics. Once the onset for H_2 desorption reaches 230 K, no further downshift is observed for Borazine/Pt(111), since this is apparently the temperature, where Borazine dehydrogenation becomes the rate-limiting step.

4. Structure of adsorbed species

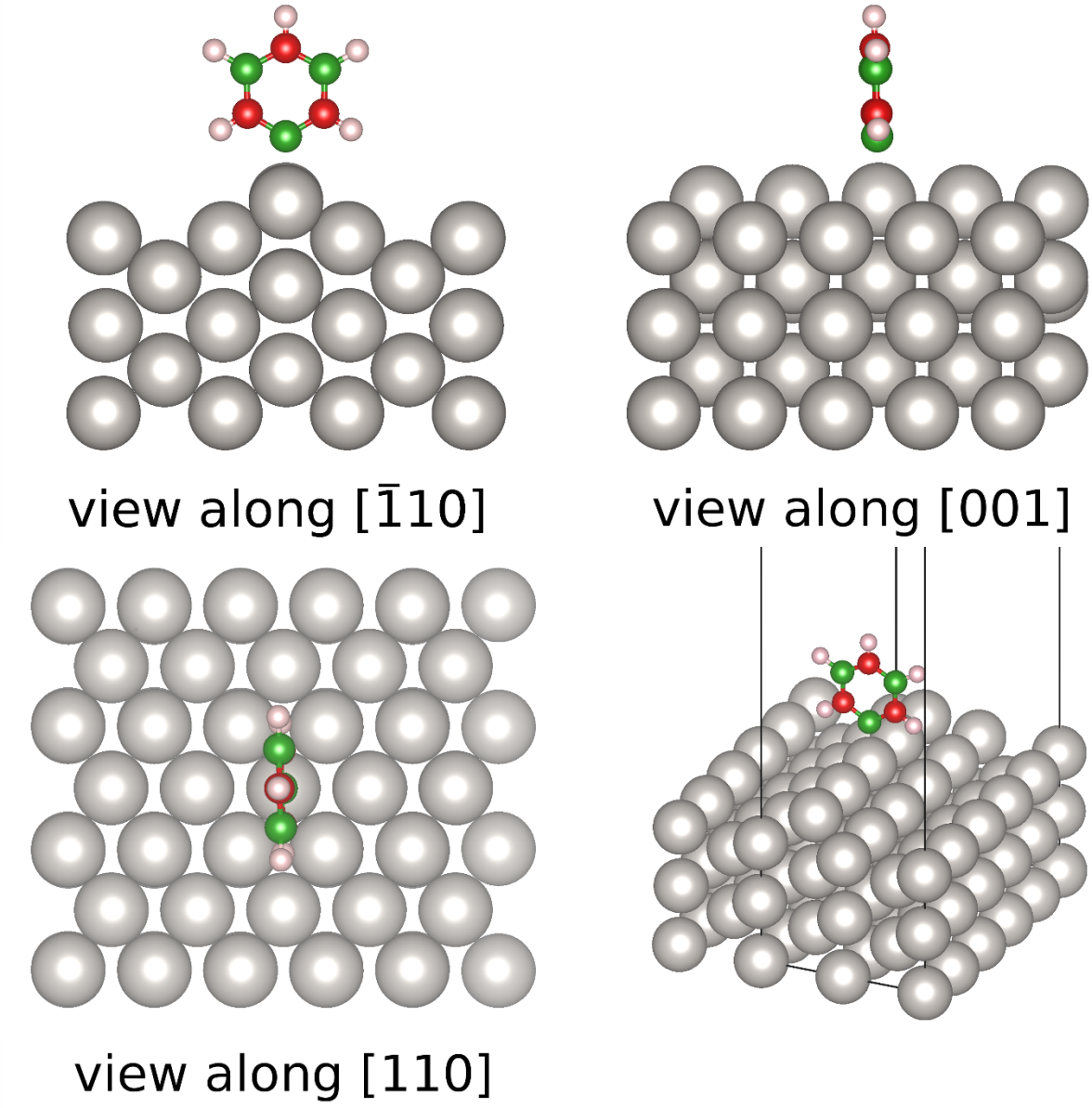

Figure S3: Structure of the B bound Borazine radical with the molecular plane oriented along [001]. The black outline of the cell is shown in the bottom right picture. Colour code: Pt grey, N red, B green, H pink.

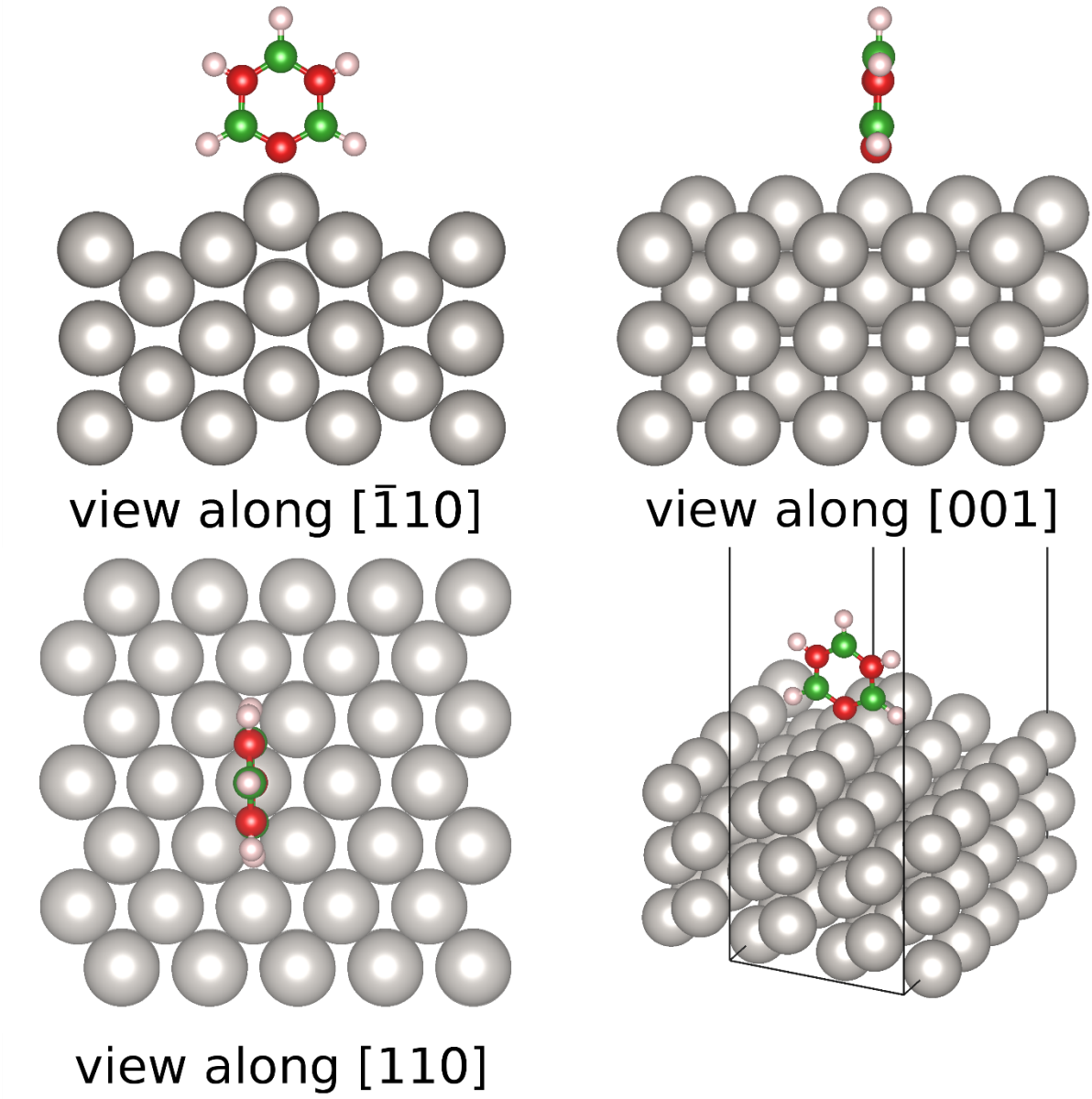

Figure S4: Structure of the N bound Borazine radical with the molecular plane oriented along [001]. The black outline of the cell is shown in the bottom right picture. Colour code: Pt grey, N red, B green, H pink.

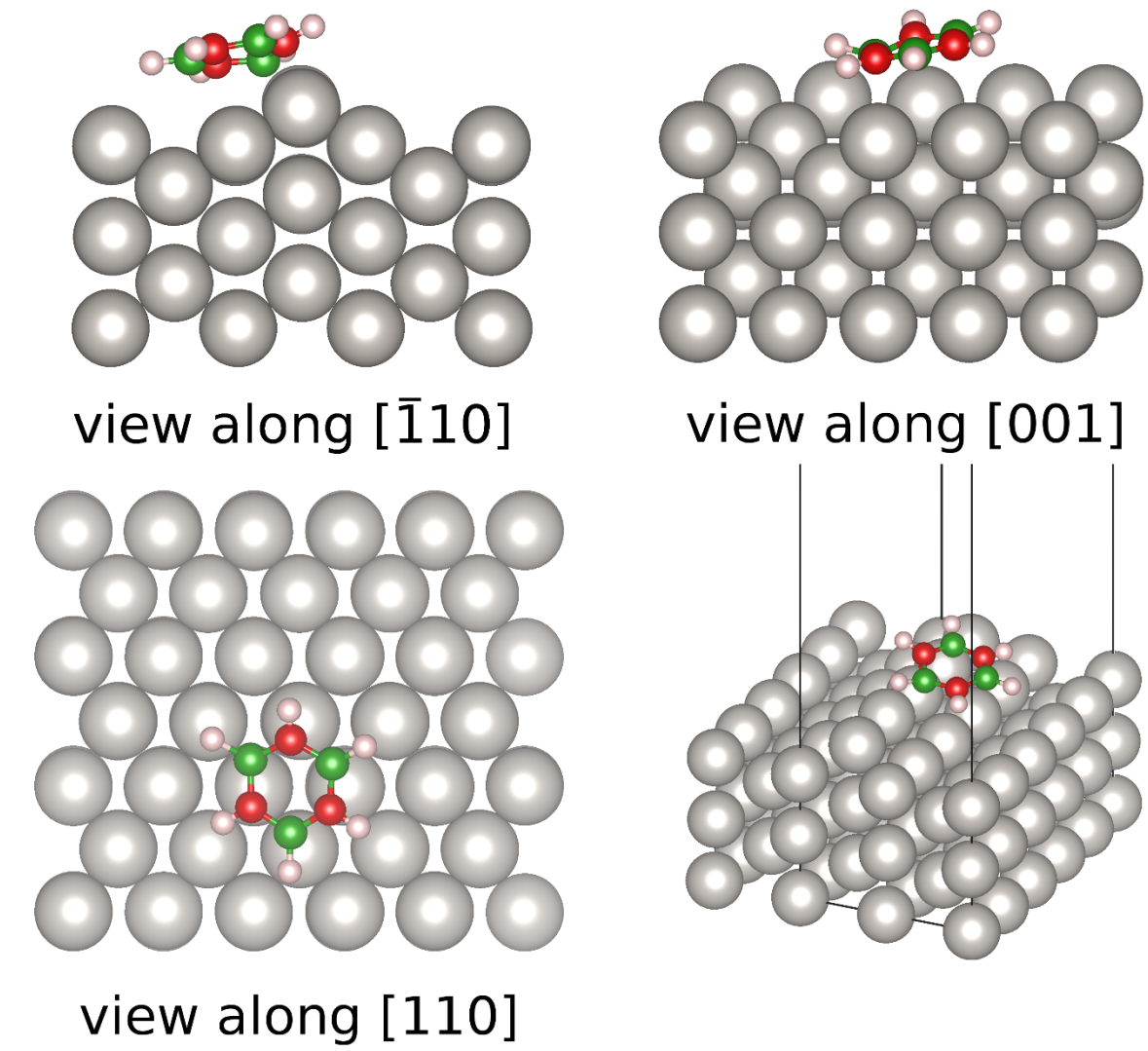

Figure S5: Structure of the molecular adsorbed borazine. The black outline of the cell is shown in the bottom left picture. Colour code: Pt grey, N red, B green, H pink.

Table ST3: Adsorption height (=B-Pt or N-Pt distance) for the Borazine radical.

	along [$\bar{1}$10]	along [001]
$(B_3N_3H_5)^{\bullet}$ via N	1.98	1.99
$(B_3N_3H_5)^{\bullet}$ via B	2.07	2.05

1 Harshbarger, W., Lee, G. H., Porter, R. F. & Bauer, S. H. Structure of borazine. *Inorganic Chemistry* **8**, 1683-1689, doi:10.1021/ic50078a023 (1969).
2 Peyerimhoff, S. D. & Buenker, R. J. Comparison of the molecular structure and spectra of benzene and borazine. *Theoretica chimica acta* **19**, 1-19, doi:10.1007/bf00527373 (1970).
3 Simonson, R. J., Paffett, M. T., Jones, M. E. & Koel, B. E. A vibrational study of borazine adsorbed on Pt(111) and Au(111) surfaces. *Surface Science* **254**, 29-44, doi:https://doi.org/10.1016/0039-6028(91)90635-6 (1991).
4 Jo, S. K. Weakly-bound hydrogen on defected Pt(111). *Surface Science* **635**, 99-107, doi:https://doi.org/10.1016/j.susc.2014.12.014 (2015).